inaccuracies [5, 6]. Evaluation of ankle–hindfoot stability under applied force, such as inversion or anterior translation, is widely performed clinically and radiologically. It is known that these evaluating methods have some limitations. Stress radiographs of the ankle measure two-dimensional displacement, but instability occurs in three planes. Moreover, in these stress evaluations and earlier studies, ankle-joint stability was investigated in discrete joint positions. However, the positions selected may or may not have been positions in which laxity was at its maximum. The optimal joint position for testing varies depending upon the specific ligament being tested. Also, most of these investigations were cadaveric studies that used methods not directly applicable to testing patients.

We developed an ankle-testing device to measure three-dimensional ankle and hindfoot motion with a specific rotational force applied and succeeded in distinguishing between controls and injured ankles and isolated the anterior talofibular ligament (ATFL) and combined ATFL/calcaneofibular ligament (CFL) laxity in vitro [7–9]. The purposes of this study were to: (1) determine the repeatability of the testing methods in vivo; (2) apply this technique to uninjured controls; (3) apply this technique to patients with chronic lateral ankle ligament instability to determine the feasibility of its use in routine clinical testing.

Materials and methods

Patient profile

Ten individuals without previous foot trauma or pathology were tested. Three were women; average age was 35 (range 26–42) years. The tests were performed three to five times on two different days in order to assess the repeatability of the method. Three patients with unilateral injuries to the lateral ligaments were also tested. Mean age was 26 (range 14–41) years. Two were women. All had chronic instability based upon physical examination with a positive anterior drawer, and all had abnormal stress radiographs. Both the unstable and stable ankles were tested in the device. All three patients had combined ATFL/CFL rupture confirmed at the time of surgery. Patients underwent reconstruction of lateral ankle ligament using the modified Broström procedure.

Ankle-stability-testing device

The ankle-testing apparatus was constructed primarily of acrylic plastic (Fig. 1). It allowed three rotations (internal/external, inversion/eversion, plantar/dorsiflexion) of the footplate and three translations (anterior/posterior, medial/lateral, proximal/distal) in a global anatomical coordinate system of the hindfoot. In this coordinate system, the X axis was along the tibial shaft through the centre of the ankle. The Z axis was parallel to the projection of a line connecting the centre of the heel and the second metatarsal on a plane perpendicular to the X axis. The Y axis was the product of the X axis and Z axis following the right-hand rule, passing through the ankle-joint centre. The X axis was defined as the internal/external rotation axis, the Z axis as the inversion/eversion axis, and the Y axis as the plantar/dorsiflexion axis. A 1.7 Nm torque was applied separately to each axis using a stainless steel, 180° torsion spring.

Each patient was placed in the apparatus in a seated position in 90° of hip and 90° of knee flexion. The lower leg was fixed on a low-friction sliding block to allow free

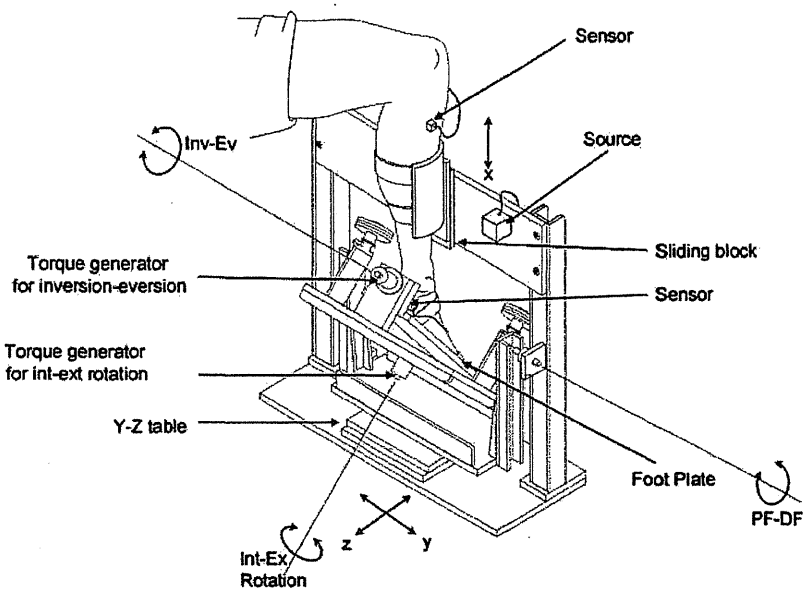

Fig. 1 Ankle-testing apparatus

proximal–distal motion of the tibia. The foot was fixed on the foot plate with a Velcro® strap on the forefoot and midfoot. The hindfoot was secured to a heel cup on the plate by a Velcro® strap. Three-dimensional movement of the calcaneus relative to the tibia (ankle–hindfoot complex) was monitored with an electromagnetic tracking system (Flock of Birds®, Ascension Technology, Burlington, VT, USA), which provided 6 degrees of freedom tracking. The magnetic source was mounted to the frame of the testing device. One sensor was attached to the skin overlying the calcaneal tuberosity, and another was attached to the anteromedial aspect of the proximal leg. Placement of sensors in these areas with less subcutaneous tissues limited the potential for artifact from skin movement. A pilot study was performed to compare kinematics data from both skin- and bone-mounted sensors using cadaver feet, which confirmed that the measurements from skin-mounted sensors correlated well with bony movements [7].

Internal rotation then inversion stresses were applied using constant loading of the foot with a built-in, spring-loaded torque generator. A constant torque of 1.7 Nm was applied, determined on the basis of previous tests and clinical experience. The foot was moved slowly from maximum plantarflexion to maximum dorsiflexion, with the constant torque applied to the foot in either internal rotation or inversion. Three-dimensional kinematic data were recorded continuously during testing. Internal/external rotation and inversion/eversion movement curves expressed as functions of the plantar/dorsiflexion angle. Internal rotation and inversion angles and the slope of the curves were determined for the unstable and the opposite stable ankle, as well as for controls. Discrete points were selected for data analysis: the angle of each curve was determined at 20° and 10° of plantarflexion, neutral position, and 10° of dorsiflexion. The slope was calculated between the points representing maximum motion and a point corresponding to motion at 10° of dorsiflexion from the internal rotation curve or the inversion curve.

Statistical analysis was performed using a paired t test to evaluate the difference between stable and unstable ankles, with statistical significance set at $p<0.05$. An unpaired t test was used to evaluate the difference between unstable ankles and controls, with statistical significance set at $p<0.05$ level.

Results

Repeatability

The technique had repeatable results. The intraclass correlation (ICC) > was 0.97 for same-day testing and 0.95 for testing on different days for the inversion stress test. For the internal rotation stress test, the ICC was 0.93 for intraday tests and 0.90 for interday tests. An example of three trials obtained from one individual is shown in Fig. 2.

Uninjured control ankles

Angular data obtained from ten controls are shown in Fig. 3. Maximum inversion was observed in a position >20° of plantarflexion and decreased as the ankle dorsiflexed. The mean ± standard deviation (SD) value of maximum inversion was 15.8°±3.7° , with a range of 8.3–22.5°. Mean value of minimum inversion was 6.6°±2.6°, with a range of 2.2–10.6°. Mean maximum to minimum inversion was 9.2°± 3.2°, with a range of 2.7–13.4°. The shape of curves for the internal rotation stress test was convex with the peak of the convex curve at an average of 7.1°±6.1° plantarflexion, ranging from 17° plantarflexion to 1° dorsiflexion. Mean value of maximum internal rotation was 15.4°±3.4°, with a range of 8.8–20.7°. Mean value of minimum internal rotation was 11.7°±3.5°, with a range of 6.5–18.2°. Mean range from maximum to minimum internal rotation was 3.7°±1.9°, with a range of 1.2–7.4°.

Unstable ankles

The motion curve patterns in unstable ankles were similar among the three patients with lateral ankle instability.

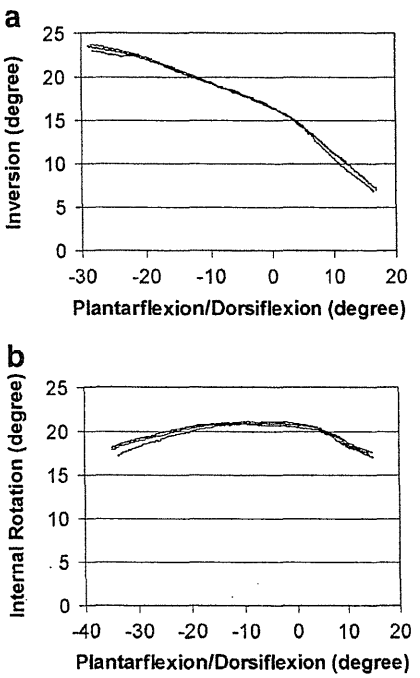

Fig. 2 Ankle–hindfoot complex motion curve of an uninjured control anke: three trials. Inversion or internal rotation motion of the ankle–hindfoot complex is expressed as a function of plantar/dorsiflexion angle. **a** Inversion stress test. **b** Internal rotation stress test

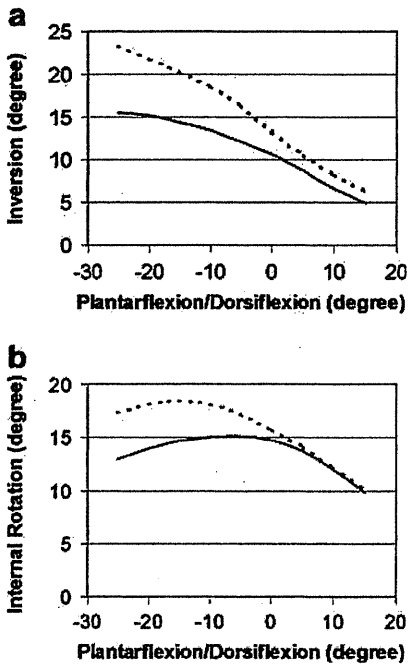

Fig. 3 Mean ankle–hindfoot complex motion showing the effect of ankle-flexion angle on the amount of inversion or internal rotation in ten uninjured controls (*solid lines*) and three patients with instability (*dotted lines*). **a** Inversion stress test. **b** Internal rotation stress test

Overall, there was more motion with inversion and internal rotation testing. The degree of rotation at five discrete points was identified and compared between the unstable and the stable ankle. These points were 20° and 10° of plantarflexion, neutral, 10° of dorsiflexion, and maximum internal rotation or inversion position. For the inversion stress test, the difference in motion curves was greatest in plantarflexion. Further analysis of the motion curve slopes was much more sensitive in differentiating between the unstable and the opposite stable ankle (Figs. 4 and 5). With internal rotation force applied, mean ± SD slope was 29.4±8.3

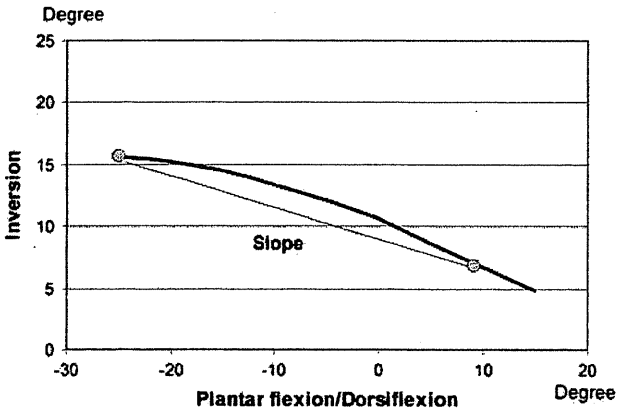

Fig. 4 Determination of slope of the motion curve from a point at 10° of dorsiflexion to a point at the peak of the motion curve

(in the unstable ankle, which was significantly greater than 11.7±5.0 in the opposite stable ankle (p=0.03). With inversion force applied, the mean ± SD slope of 44.8±11.4 in the unstable ankle was significantly different than that of 20.7±2.4 in the opposite stable ankle (p=0.04). Similarly, slopes of the inversion and internal rotation motion curves were significantly greater in unstable ankles than in uninjured controls (Fig. 5).

Discussion

Stress radiography with anterior drawer or inversion stress is widely accepted as a means to assess patients with lateral ankle ligament injuries. Anterior talar displacement or talar tilt angle is measured under stress loading. However, accuracy of these conventional stress tests is suspect [4–6, 10–15]. Some limitations in the standard evaluation methods were because ankles were tested in various

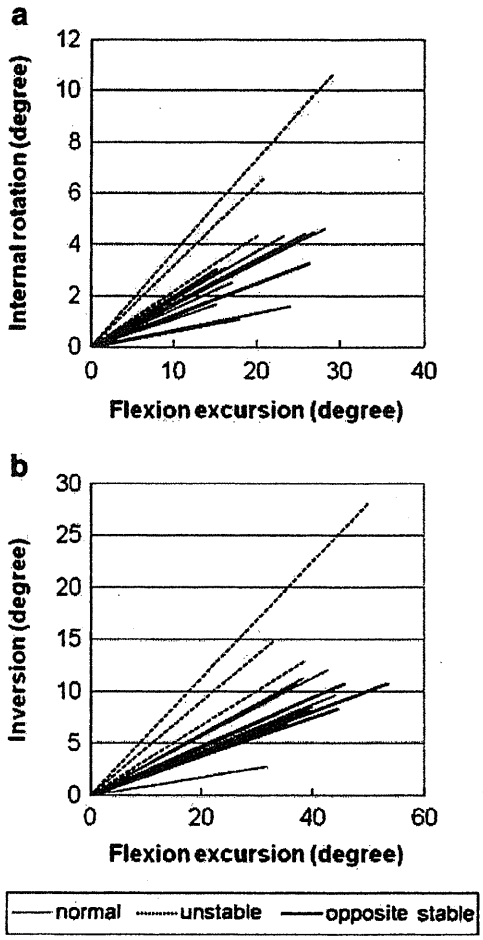

Fig. 5 Slopes from motion curves in three unstable ankles (*dotted lines*), their opposite stable ankles (*solid black lines*), and ten uninjured controls (*solid gray lines*). **a** Internal rotation stress test. **b** Inversion stress test

positions and with different forces applied. Different authors recommended stressing the ankle in dorsiflexion, in the neutral position, or in plantarflexion during the stress manoeuvre [6, 10, 16, 17]. The foot position affects ankle stability because the relationship between ligamentous laxity and bony constraints vary with flexion angle during stress testing [7, 9, 18–21]. Our results showed that mobility of the ankle–hindfoot complex varied as foot flexion angle changed. The magnitude of inversion increased with increasing plantarflexion position of the ankle under inversion stress.

The diagnostic method in this study is based upon foot-motion measurements under different specific manipulations and analysis of motion curve patterns using trend analysis [9]. This can be a fundamental improvement over the existing stress testing, which depends upon a discrete one-point value to determine laxity and type of injury. Each ligament contributes to joint stability at a certain joint position, and the rupture of a ligament will cause instability at that position. Thus, comparison based on the overall curve trend should be more sensitive than using discrete points in evaluating ligament injury. The existing testing analyses rotation in one plane (inversion) or translation in one direction (anterior drawer) but does not consider other planes of rotation or displacement, such as internal rotation. It may be reasonable to measure internal rotation to diagnose ATFL injury because the ATFL functions primarily in restricting internal rotation of the talus in the mortise [22]. Although this device may be applicable to stress radiography, we think that the motion-curve analysis during full range of sagittal motion will provide more detailed information of ankle–hindfoot complex kinematics and lead to more accurate diagnosis of severity of ankle ligament injuries.

We calculated slopes from the motion curves and applied them to differentiate between unstable (combined ATFL and CFL rupture) and stable ankles because a previous in vitro study demonstrated that it was possible to differentiate simulated ATFL injury from an intact ankle and ATFL/CFL injury from ATFL injury with this method [9]. Further study is needed of patients who have persistent ankle pain after sprains in order to determine whether these distinctions can be made in vivo; such analysis is not possible with conventional stress tests. Also, there is a subset of patients with persistent pain after ankle ligament reconstruction or after injury who have negative stress radiographs and stable ankles on examination who are considered to have "functional instability." Perhaps the diagnoses of some of these patients can be clarified with the testing method described here. We tested patients with inversion or internal rotation force applied. However, with the testing device, it is also possible to apply constant eversion, external rotation, combined inversion/internal rotation, and eversion/external rotation stress to the ankles. It may therefore be an applicable assessment for patients with other diagnoses, such as suspected deltoid ligament instability.

Although this is a promising noninvasive method of differentiating ankle ligament instabilities, there are limitations. We found variability in absolute values of inversion or internal rotation measured between patients. It is well recognised that there is wide variation among individuals in stress tests [6, 12, 13, 23], which our testing confirmed. This observation in preliminary testing led to refinements in how the foot was secured to the footplate, standardising a neutral position prior to testing, and the repeatability study that was conducted. Data analysis was time consuming, and a special device to measure continuous three-dimensional movement is needed. Some modifications will be required when this device is considered as a widely used examination tool in clinical settings.

Patients with unstable ankles were differentiated from uninjured controls by using the ankle-stability-testing device. The method is noninvasive, does not involve radiation exposure, and is repeatable. It has the potential of providing more accurate diagnosis of ankle-ligament injuries.

Acknowledgements The authors gratefully acknowledge the support by the National Institutes of Health (AR44035) and the assistance from Denny J. Padgett, P.T.

Conflict of interest The authors declare that they have no conflict of interest.

References

1. Waterman BR, Owens BD, Davey S, Zacchilli MA, Belmont PJ Jr (2010) The epidemiology of ankle sprains in the United States. J Bone Joint Surg Am 92:2279–2284. doi:10.2106/JBJS.I.01537
2. Thacker SB, Stroup DF, Branche CM, Gilchrist J, Goodman RA, Weitman EA (1999) The prevention of ankle sprains in sports. A systematic review of the literature. Am J Sports Med 27:753–760
3. Yeung MS, Chan KM, So CH, Yuan WY (1994) An epidemiological survey on ankle sprain. Br J Sports Med 28:112–116
4. Karlsson J, Lansinger O (1992) Lateral instability of the ankle joint. Clin Orthop Relat Res:253–261
5. Frost SC, Amendola A (1999) Is stress radiography necessary in the diagnosis of acute or chronic ankle instability? Clin J Sport Med 9:40–45
6. Fujii T, Luo ZP, Kitaoka HB, An KN (2000) The manual stress test may not be sufficient to differentiate ankle ligament injuries. Clin Biomech (Bristol, Avon) 15:619–623. doi:S0268-0033(00)00020-6
7. Fujii T, Kitaoka HB, Luo ZP, Kura H, An KN (2005) Analysis of ankle-hindfoot stability in multiple planes: an in vitro study. Foot Ankle Int 26:633–637. doi:894987
8. Fujii T, Kitaoka HB, Watanabe K, Luo ZP, An KN (2006) Comparison of modified Brostrom and Evans procedures in simulated lateral ankle injury. Med Sci Sports Exerc 38:1025–1031. doi:10.1249/01.mss.0000222827.56982.40

9. Fujii T, Kitaoka HB, Watanabe K, Luo ZP, An KN (2010) Ankle stability in simulated lateral ankle ligament injuries. Foot Ankle Int 31:531–537. doi:10.3113/FAI.2010.0531
10. Bahr R, Pena F, Shine J, Lew WD, Lindquist C, Tyrdal S, Engebretsen L (1997) Mechanics of the anterior drawer and talar tilt tests. A cadaveric study of lateral ligament injuries of the ankle. Acta Orthop Scand 68:435–441
11. Becker HP, Komischke A, Danz B, Bensel R, Claes L (1993) Stress diagnostics of the sprained ankle: evaluation of the anterior drawer test with and without anesthesia. Foot Ankle 14:459–464
12. Cass JR, Morrey BF, Chao EY (1984) Three-dimensional kinematics of ankle instability following serial sectioning of lateral collateral ligaments. Foot Ankle 5:142–149
13. Glasgow M, Jackson A, Jamieson AM (1980) Instability of the ankle after injury to the lateral ligament. J Bone Joint Surg Br 62-B:196–200
14. Johannsen A (1978) Radiological diagnosis of lateral ligament lesion of the ankle. A comparison between talar tilt and anterior drawer sign. Acta Orthop Scand 49:295–301
15. Larsen E (1986) Experimental instability of the ankle. A radiographic investigation. Clin Orthop Relat Res:193–200
16. Grace DL (1984) Lateral ankle ligament injuries. Inversion and anterior stress radiography. Clin Orthop Relat Res:153–159
17. Lahde S, Putkonen M, Puranen J, Raatikainen T (1988) Examination of the sprained ankle: anterior drawer test or arthrography? Eur J Radiol 8:255–257
18. Allinger TL, Engsberg JR (1993) A method to determine the range of motion of the ankle joint complex, in vivo. J Biomech 26:69–76. doi:0021-9290(93)90614-K
19. Blanshard KS, Finlay DB, Scott DJ, Ley CC, Siggins D, Allen MJ (1986) A radiological analysis of lateral ligament injuries of the ankle. Clin Radiol 37:247–251. doi:S0009-9260(86)80328-2
20. Hollis JM, Blasier RD, Flahiff CM (1995) Simulated lateral ankle ligamentous injury. Change in ankle stability. Am J Sports Med 23:672–677
21. Kovaleski JE, Gurchiek LR, Heitman RJ, Hollis JM, Pearsall AWT (1999) Instrumented measurement of anteroposterior and inversion-eversion laxity of the normal ankle joint complex. Foot Ankle Int 20:808–814
22. Rasmussen O (1985) Stability of the ankle joint. Analysis of the function and traumatology of the ankle ligaments. Acta Orthop Scand Suppl 211:1–75
23. Lapointe SJ, Siegler S, Hillstrom H, Nobilini RR, Mlodzienski A, Techner L (1997) Changes in the flexibility characteristics of the ankle complex due to damage to the lateral collateral ligaments: an in vitro and in vivo study. J Orthop Res 15:331–341. doi:10.1002/jor.1100150304

Clinical Biomechanics 27 (2012) 189–195

Contents lists available at SciVerse ScienceDirect

Clinical Biomechanics

journal homepage: www.elsevier.com/locate/clinbiomech

The role of ankle ligaments and articular geometry in stabilizing the ankle

Kota Watanabe [a], Harold B. Kitaoka [b], Lawrence J. Berglund [b], Kristin D. Zhao [b], Kenton R. Kaufman [b], Kai-Nan An [b,*]

[a] Department of Orthopaedic Surgery, Sapporo Medical University School of Medicine, South-1, West-16, Chuoku, Sapporo, Hokkaido, 060-8543, Japan
[b] Orthopedic Biomechanics Laboratory, Department of Orthopedic Surgery, Mayo Clinic, 200 First Street SW, Rochester, MN 55905, USA

ARTICLE INFO

Article history:
Received 11 February 2011
Accepted 26 August 2011

Keywords:
Ankle
Stability
Ligaments
Biomechanics
Cadaver

ABSTRACT

Background: Ankle joint stability is a function of multiple factors, but it is unclear to what extent extrinsic factors such as ligaments and intrinsic elements such as geometry of the articular surfaces play a role. The purposes of this study were to determine the contribution of the ligaments and the articular geometry to ankle stability and to determine the effects of ankle position and simulated physiological loading upon ankle stability.
Methods: Sixteen cadaveric lower extremities were studied in unloaded and with axial load equivalent to body weight. Anterior–posterior, medial–lateral translation and internal–external rotation tests were performed in neutral, dorsiflexion and plantarflexion ankle positions. Intact ankle stability was measured; ankle ligaments were serially sectioned and retested.
Findings: For unloaded condition, the lateral ligament accounted for 70% to 80% of anterior stability and the deltoid ligaments for 50% to 80% of posterior stability. Both ligaments contributed 50% to 80% to rotational stability; however, the ligaments did not provide the primary restraints to medial–lateral stability. For loaded ankle condition, articular geometry contributed 100% to translational and 60% to rotational stability. The ankle was less stable in plantarflexion and more stable in dorsiflexion.
Interpretation: The contribution of extrinsic and intrinsic elements to ankle stability is dependent upon the load and direction of force applied. This study underscores the importance of restoring soft tissues about the ankle to the anatomic condition during reconstruction operations for instability, trauma and arthritis.

1. Introduction

The ankle joint is affected by a variety of disorders such as sprains, fractures and arthritis (Mack, 1982; Yeung et al., 1994). The estimated incidence rate of ankle sprains in the general population presenting to emergency departments in the United States is 2.15 per 1000 person-years (Waterman et al., 2010). In the sports field, ankle sprains account for 20% to 25% of all time-loss injuries in running or jumping sports such as basketball, football, soccer, field hockey and volleyball (Mack, 1982). Twisting of the ankle under load may cause ankle fractures, ligamentous injuries, or both. Specific injuries depend on several factors such as weightbearing, orientation of the forces involved, or stabilizing roles of ankle structures.

Biomechanical studies have been performed on the ankle joint, specifically focusing on ankle stability. Ankle stability is a function of both extrinsic elements such as ligaments and intrinsic elements such as geometry of the articular surface. The contribution of extrinsic factors has been studied in joints (Butler et al., 1980; Itoi et al., 2000; Knutson et al., 2000; Minami et al., 1985; Morrey and An, 1983; Ritt et al., 1998) including the ankle (Stormont et al., 1985; Tochigi et al., 2006). A previous study reported contribution of the ligaments and articular surface in the ankle to rotation and version stability, but did not include translational stability (Stormont et al., 1985). Another study reported contribution of the articular surface geometry to ankle stability, but did not include ligamentous contribution (Tochigi et al., 2006). There is still uncertainty about the effects of weightbearing, different ankle positions and soft tissue integrity upon ankle stability, as well as the contribution of intrinsic factors such as joint geometry. With lower levels of loading of the ankle, it is presumed that ligamentous structures function as more dominant stabilizers. As axial load increases, the contribution of the articular geometry to stability is presumed to increase. These relationships are relevant to understanding the mechanisms of joint injury, as well as surgical interventions such as ligament reconstruction and arthroplasty.

Methods for measuring intrinsic joint stability as well as ligamentous contributions have been reported from this laboratory in various joints (Berglund et al., 1994; Halder et al., 2001; Haugstvedt et al., 2002; Itoi et al., 2000; Stuart et al., 2000), and established in the ankle joint (Watanabe et al., 2009). The purpose of this study was to determine the contribution of the deltoid and lateral ankle ligaments as well as articular geometry to stability of the ankle joint and to determine the effects of ankle position and simulated physiological loading upon ankle stability.

* Corresponding author at: Mayo Clinic, Department of Orthopedic Surgery, 200 First Street SW, Rochester, MN 55905, USA.
E-mail address: an@mayo.edu (K.-N. An).

0268-0033/$ – see front matter © 2011 Elsevier Ltd. All rights reserved.
doi:10.1016/j.clinbiomech.2011.08.015

2. Methods

There were two parts of the study. In the first part, sixteen normal (uninjured), fresh-frozen human cadaveric lower extremities donated from 13 individuals without foot–ankle pathology were studied. The mean age of the specimens was 72 years (range, 61 to 83 years). Fourteen specimens were male and two were female. Eight were right feet and eight were left feet. In the second part, eight specimens donated from 6 individuals were tested under simulated ankle ligament injury conditions. Seven specimens were male and one was female. Six were right feet and two were left feet. The specimens were disarticulated at the knee and at the mid-tarsal joints. Soft tissues including skin, subcutaneous tissues and muscles were dissected, maintaining all ligaments and the interosseous membrane intact. The subtalar joint was immobilized by Steinmann pins and hindfoot potted in polymethylmethacrylate (PMMA) cement in the neutral position. The institutional research ethics committee reviewed and approved the study.

The testing device provided simultaneous measurement of multi-axis loading and displacements of the talus relative to the tibia (Fig. 1). The device was designed in order to allow for testing in multiple planes without removing or repositioning the specimens for various directions of translation. It was designed to permit operative procedures to be performed without unmounting and remounting the specimen for each testing condition, thus reducing the potential for artifact. The tibia, but not the fibula, was potted and fixed to the testing frame to permit tibiofibular motion. A 6-component load cell (AMTI, Newton, MA, USA) was used to measure forces and moments. The hindfoot (talus, calcaneus) was potted in a rectangular metal fixture. This fixture was attached to two *X–Y* motorized horizontal stages for applying medial–lateral (ML) and anterior–posterior (AP) translation forces and a motorized rotary stage for applying internal or external rotation motions. An additional low friction *x–y* positioning slide was placed beneath the motorized stages to allow for proper positioning of the hindfoot relative to the tibia and to minimize any constraint in specific axis during the testing regimen. During AP translation testing, the AP positioning slide was locked, but ML translation was unconstrained. During ML translation testing, the ML positioning slide was locked, but AP translation was unconstrained. During rotation testing, both AP and ML positioning slides were released to allow unconstrained pure moments about that axis. Linear potentiometers (Novotechnik, Southborough, MA) were used to measure translational displacements at the joint level and were affixed between the potted hindfoot and distal tibia. Internal–external rotation (adduction, abduction) of the ankle was measured with a rotatory potentiometer incorporated in the motorized rotary stage. Internal–external rotation occurred about the axis along the tibial shaft which was perpendicular to the *X–Y* horizontal stage.

Motor control and data acquisition were accomplished with Labview software (National Instruments, Austin, TX, USA). The frame to which the tibia was attached was clamped onto a low-friction vertical slide. The tibia was suspended to this frame with multiple heavy threaded Steinman pins, but the fibula was not fixed, in order to permit physiological tibio-fibular motion. Two axial loading conditions were tested: a minimal level (5 N) and approximately body weight (700 N) through this slide by a low-friction pneumatic cylinder (Illinois Pneumatic, Roscoe, IL, USA). The ankle bears high levels of compressive forces during normal level walking (Simonsen et al., 1995), but in preliminary experiments, we found that repeated testing of anatomic specimens at high loading levels could alter the soft tissue and bony anatomy. In a pilot study, ankles were tested in 100 N axial load increments up to 1000 N and we found that the load–displacement characteristics of the talus relative to the tibia became consistent at the 600 N level and higher. Therefore, 700 N was chosen as the simulated physiological axial loading of body weight. Axial loads of 5 N (essentially unloaded) and 700 N (loaded) were applied in each of three ankle positions: 15° of plantarflexion, neutral and 10° of dorsiflexion. These angles represented the range of sagittal ankle motion during the stance phase of gait. Experimentally, these positions were consistently obtained by inserting a wedge (10° or 15°) under the ankle fixture.

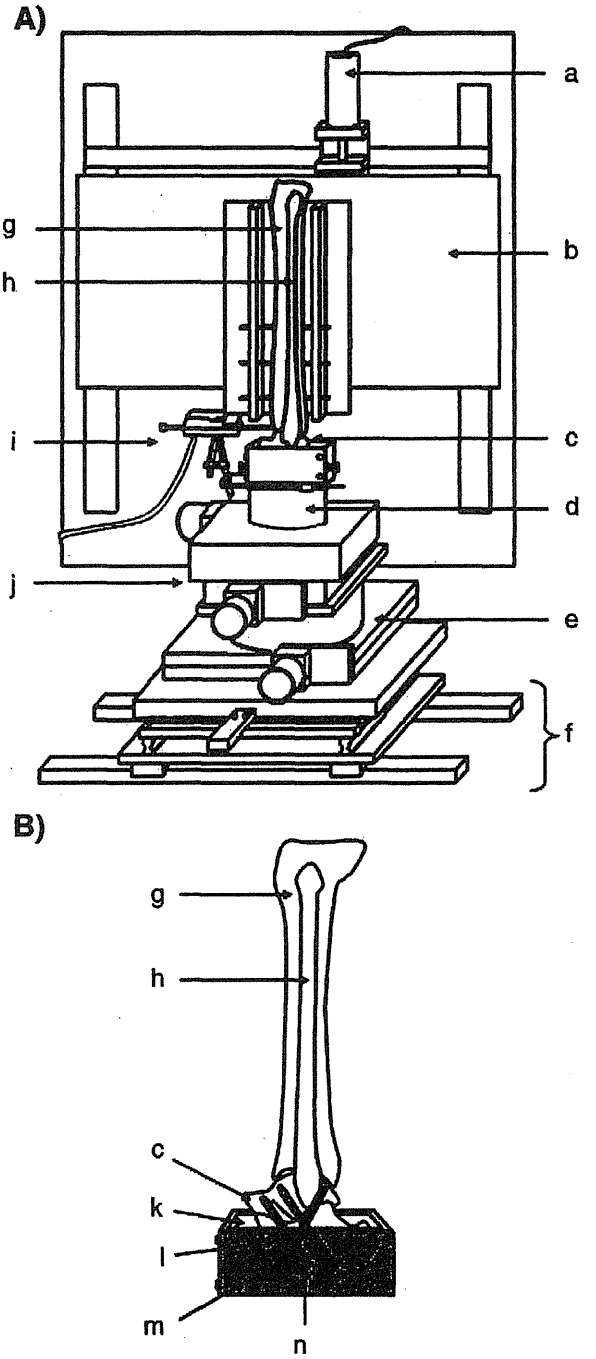

Fig. 1. Multi-axis materials testing machine: A, testing device; B, lower extremity specimen embedded in PMMA. a) Axial load actuator, b) low-friction vertical slide, c) talus, d) six component load cell, e) motorized rotary stage, f) positioning stage, g) tibia, h) fibula, i) potentiometer, j) motorized horizontal stage, k) polymethylmethacrylate, l) calcaneus, m) potting fixture (gray), n) Steinmann pins. The tibial shaft was fixed perpendicular to the *X–Y* horizontal stage (j) and internal–external rotation was about the axis along the tibial shaft.

All anatomic specimens were tested in the normal, intact condition for the first part of the study. In the second part, further testing was performed in eight feet. In four feet, the deltoid ligament was sectioned first and testing repeated, then the lateral ankle ligaments

were sectioned and testing performed. In another four feet, the lateral ankle ligaments were sectioned and testing performed, then the deltoid ligament and testing completed. The tibiofibular syndesmosis, anterior tibiofibular and posterior tibiofibular ligaments proximally and distally were left intact in order to permit free movement between the tibia and fibula.

Translation tests consisted of anterior, posterior, medial and lateral translation of the talus at a rate of 2 mm per second. Translation was described relative to the global horizontal rather than to the foot's local segment horizontal. When the ankle was dorsiflexed and plantarflexed, the anterior–posterior translation was determined with respect to the global horizontal or the *X–Y* plane of the testing apparatus. For intact specimens, after a load limit of 150 N in the direction of motion was reached, the direction was reversed and testing completed. For initial rotation testing of intact specimens, internal or external rotation torque was applied to the talus at a rate of 2 degrees per second up to the torque limit of 2.5 Nm. After the ligament sectioning, these tests were repeated; however translational and rotational displacement values were used as endpoint limits for each specimen. The limits for translation tests were determined as the displacement in each direction corresponded to that measured under 150 N of load in the intact condition. The limits of rotation corresponded to that measured at 2.5 Nm of torque in the intact specimen.

2.1. Data analysis

Testing conditions included the intact foot, sectioning the lateral ligaments or deltoid ligament and sectioning both ligaments in each of the three ankle positions (15° of plantarflexion, neutral and 10° of dorsiflexion). All tests were performed for both the 5 N (unloaded) and 700 N (loaded) axial load conditions. Load–displacement curves were obtained from the intact, one ligament sectioned and both ligaments sectioned conditions. An example is seen in Fig. 2. The corresponding forces at the predetermined displacement values were derived from each curve. Relative contributions of the sectioned ligaments to joint stability were expressed as a percentage and calculated as the reduction in load from the intact, divided by the intact load value. Contribution of articular geometry to joint stability was expressed as a percentage and calculated as the remaining load after both ligaments were sectioned, divided by the intact load value. For the purposes of this study, we defined a primary restraint structure as one that provides more than 50% of restraint to translation or rotation.

Statistical analysis was performed with repeated measures ANOVA and Friedman test. The level of significance was set at $P<0.05$. Significant main effects were further analyzed using the Student–Newman–Keuls multiple comparisons test.

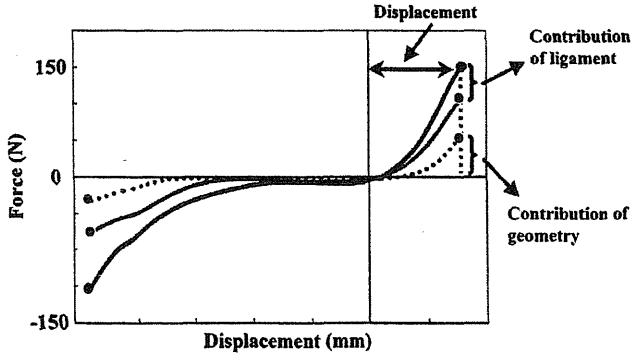

Fig. 2. Typical force–displacement curve in 5 N axial loading condition. The solid line represents the intact condition, the gray line represents one ligament sectioned and dotted line represents both ligaments sectioned. Tibiotalar displacement and contribution supporting elements are shown.

3. Results

The average and standard deviation of the absolute values measured at the talus at prescribed maximum load or torque values for all movement directions for the intact foot condition are shown in Fig. 3. Ankle position altered laxity of the ankle. The plantarflexed position was less stable and the dorsiflexed position most stable. With the unloaded ankle in plantarflexion, there was more movement in posterior, medial and lateral displacement as well as internal rotation than in dorsiflexion. In the dorsiflexion position, there was less posterior, medial and lateral displacement, as well as external and internal rotation than neutral position.

The effects of ankle position were also apparent when the ankles were loaded. With the loaded ankle in plantarflexion, there was more movement in medial and lateral displacement as well as internal and external rotation than in dorsiflexion. In the dorsiflexion position, there was less lateral displacement, as well as external and internal rotation than neutral position.

The relative contributions of the ligaments and the articular geometry to joint stability are shown in Figs. 4 and 5. In the unloaded ankle, the lateral ligaments were the primary restraint to anterior translation with the relative contribution ranging from 71% to 81%. The primary restraint to posterior translation was the deltoid ligament, with relative contribution ranging from 50% to 80%. The contribution of the deltoid ligament was significantly higher in plantarflexion than in dorsiflexion ($P<0.05$). For medial–lateral translation, neither of the two ligaments served as a primary restraint. For internal–external rotation, both the lateral and the deltoid ligaments contributed in stabilizing the ankle, The contribution of the deltoid ligament to external rotation was significantly lower in dorsiflexion than in neutral and plantarflexion ($P<0.05$).

The effect of ankle loading and articular geometry was apparent with testing after sectioning one or both ankle ligaments. The loaded ankle remained stable after ligament sectioning in anterior–posterior and medial–lateral translation with little change in the load displacement curves. Similarly, the loaded ankle remained stable with rotation. The articular geometry was the primary restraint with relative contributions ranging 50% to 74% (Fig. 5). We were unable to detect a difference in relative contribution between the three ankle positions.

4. Discussion

The contribution of extrinsic and intrinsic elements to ankle stability was dependent upon the load level, direction of forces applied and ligament integrity. We found that the ankle in dorsiflexion was more stable in the majority of the conditions tested. The plantarflexed ankle was the least stable. The articular geometry was the primary stabilizer of the ankle joint for simulated physiological loading. The lateral ankle ligaments were primary restraints in anterior translation, the deltoid ligament was most important in stabilizing posterior translation and both ligaments provided rotatory stability.

The present study represents a more critical analysis of the supporting elements of the ankle. We tested specimens under multiple loading conditions whereas some previous studies were conducted with a single loading condition. Previous studies did not specifically examine the effects of ankle position. Others examined rotatory stability but not translation stability. In the current study, we first determined the degree of laxity in the intact specimens, then used this limit in the testing of the injured conditions, in order to avoid damaging the remaining soft tissue constraints. In addition, the design of the testing device facilitated multi-axis testing without removing and repositioning the specimens repeatedly.

In previous studies, the range of applied forces to the ankle for translation tests varied from 50 N to 150 N (Hollis et al., 1995; Johnson and Markolf, 1983). Several of the previous biomechanical studies did not utilize the entire lower leg. In this study, the lower limb was

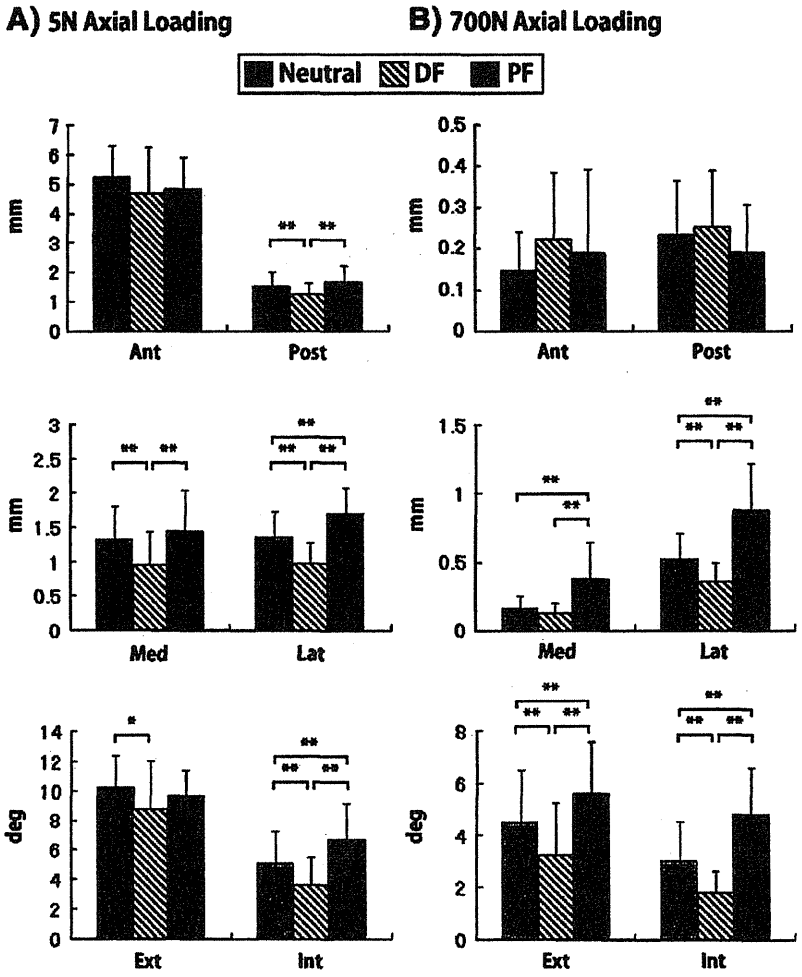

Fig. 3. Tibiotalar translation and rotation under A) 5 N axial load and B) 700 N axial load. Neutral, dorsiflexed (DF) and plantarflexed (PF) positions. (Statistically significant differences, *, $P<0.05$; **, $P<0.01$.)

utilized, maintaining motion between the tibia and fibula. Several studies reported that the fibula had apparent motion in all planes when loaded and therefore it is important to preserve the entire lower leg for testing (Barnett and Napier, 1952; Close, 1956; Stiehl, 1991). Recent investigations (Bahr et al., 1997; Cass and Settles, 1994; Hollis et al., 1995; Stiehl et al., 1993) applied these conditions to ankle stability tests and we believe they are more physiological.

Several investigators studied the range of anterior–posterior translation motion at the ankle. Hollis et al. (1995) reported 7.5 mm of anterior–posterior displacement for 50 N applied load in the neutral ankle position for anterior–posterior translation. Johnson and Markolf (1983) reported 6.6 mm of anterior–posterior displacement for 100 N and Bulucu et al. (1991) reported 6.4 mm of anterior displacement for 150 N. No axial load was applied to the ankle in any of these studies. These reported values of anterior–posterior translation were similar to our results. The effect of ankle position on anterior–posterior laxity measurements differed among investigators. Dorsiflexion was the most stable position in all three studies described above. However, Johnson and Markolf(1983) and Bulucu et al. (1991) found that the neutral position was associated with the greatest laxity, while Hollis et al. (1995) demonstrated greatest anterior–posterior laxity that in plantarflexion. In the current study, posterior displacement was significantly reduced in the dorsiflexed ankle compared to the neutral and plantar flexed positions.

There are few previous reports that studied medial–lateral translation at the ankle. In our study, the plantarflexed ankle position had significantly more medial–lateral motion than the dorsiflexed position. The geometry of the talus may be responsible for some of these differences. The width difference between the anterior (wider) and posterior (narrower) portions of the superior surface of the talar body was reported to average 2.4 mm (Stiehl, 1991). Our data reflected a significant difference in medial–lateral translation between plantar and dorsiflexed ankle positions. For internal–external rotation testing of the ankle, Johnson and Markolf (1983) reported a combined 13.8° of rotation at 2.5 Nm torque in neutral position with no axial load. McCullough and Burge (1980) reported a combined 24° for a 3 Nm torque limit with 9.8 N axial load. These values were consistent with our results of a combined 16.1° for 2.5 Nm at 5 N axial load for the neutral ankle position. Dorsiflexion was the most stable position for internal–external rotation in the current study, which was consistent with other reports (Johnson and Markolf, 1983; Stiehl et al., 1993).

Earlier reports investigated the biomechanics of lateral ligaments of the ankle. Both for *in vitro* and *in vivo* studies, rupture of the lateral ligament resulted in significant increases in anterior laxity (Bulucu et al., 1991; Glasgow et al., 1980; Hollis et al., 1995; Larsen, 1986). These findings supported our results in which the lateral ligaments contributed approximately 75% constraint to anterior translation. The deltoid ligament has not been investigated as thoroughly, especially for its effect on translational stability. Harper reported that the deltoid ligament was a secondary restraint against anterior talar translation when no axial load was applied (Harper, 1987, 1990). Our findings

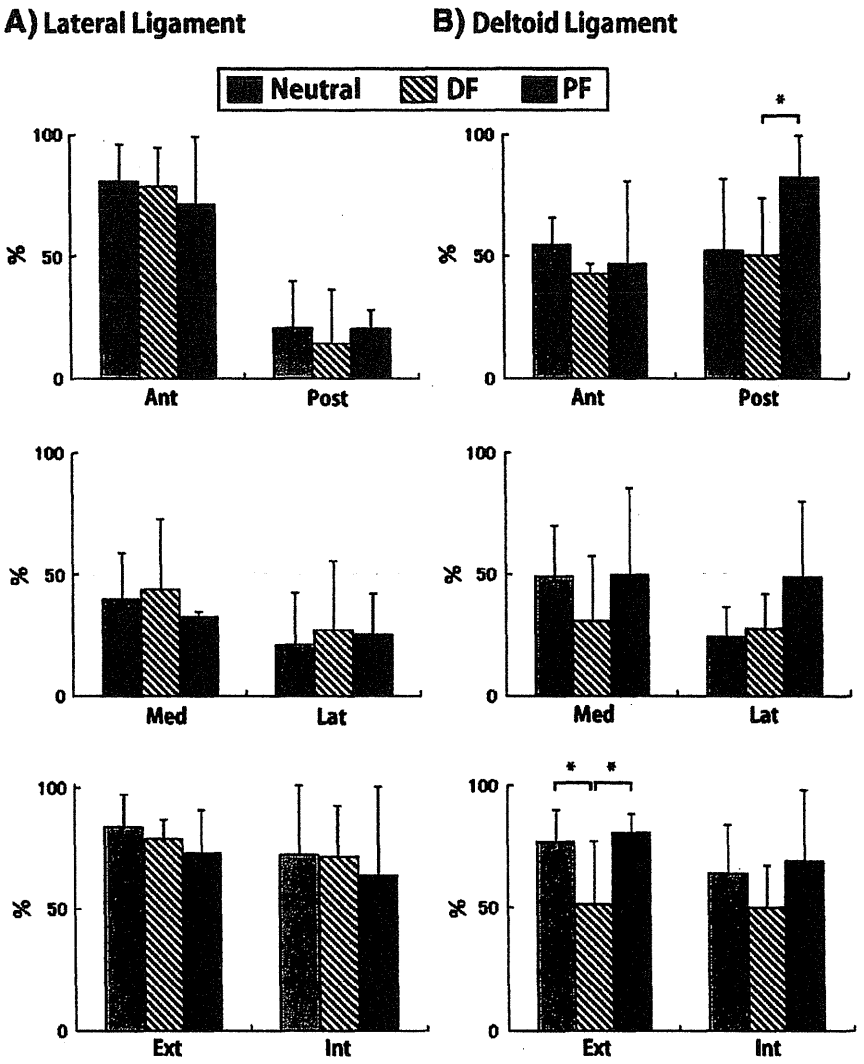

Fig. 4. Contributions of A) lateral and B) deltoid ligaments to ankle joint stability, 5 N load. Primary restraints provide more than 50% of the stability in a given condition. (Statistically significant differences, *, $P<0.05$.)

were consistent and the deltoid ligament contributed approximately 45% of the restraint to anterior translation. However, Harper also reported that posterior instability of the ankle did not increase after division of the deltoid ligament, contrary to our findings. We determined that the deltoid ligament was the primary restraint to posterior translation for the unloaded ankle. He measured the maximum amount of direct talar excursion with a caliper (0.5 mm increments) during manual stress, but the magnitudes of the applied forces were not described for each test. As Fig. 2 demonstrates, the force and stiffness decreased after ligament sectioning. If further force was applied, an increase in posterior displacement would be expected.

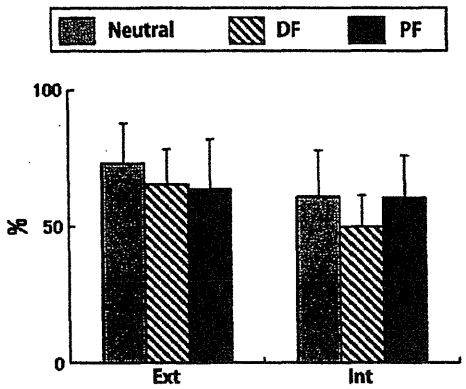

Fig. 5. Contribution of articular geometry to rotation stability of ankle joint, 700 N load.

During internal–external rotation, both the lateral and deltoid ligaments were responsible for restricting both directions of rotation for the unloaded ankle. If either of the ligaments were ruptured, rotational stability would be greatly reduced. Stormont et al. (1985) demonstrated the effect of serial sectioning of the ankle ligaments for the unloaded ankle for 3 ankle positions (plantarflexion, neutral and dorsiflexion). For internal rotation, the anterior talofibular ligament was the primary restraint in the plantar ankle position and the deltoid ligament was the primary restraint for the neutral and dorsiflexed position. For external rotation, the calcaneofibular ligament was the primary restraint for all three ankle positions. Rasmussen et al. studied the function of specific components of the lateral and deltoid ligaments (Rasmussen, 1985; Rasmussen et al., 1983). They reported that for the lateral ligaments, the anterior talofibular ligament primarily restricted internal rotation and combined cutting of the calcaneofibular and posterior talofibular ligament resulted in an increased

external rotation. For the deltoid ligament, the anterior and intermediate tibiotalar ligaments, in combination, controlled both external and, together with the anterior talofibular ligament, internal rotation of the talus. These studies suggested that cooperative function of both the lateral and deltoid ligaments was essential to provide internal and external rotation stability of the talus in the ankle mortise.

Under simulated physiologic loading (700 N), the articular surface accounted for 100% of stability in translation and 60% in external–internal rotation. Several studies support the importance of axial load for ankle stability (Glasgow et al., 1980; Liu et al., 2000; McCullough and Burge, 1980; Rasmussen, 1985; Stiehl et al., 1993; Stormont et al., 1985; Tochigi et al., 2006). Stiehl et al. (1993) tested two axial loading conditions and showed that increased axial load increased stability. Anterior–posterior translation at a 150 N translation force was 8 mm during a 147 N axial load and reduced significantly to 4 mm with an increased axial load of 686 N. Two other cadaver studies reported articular contribution to ankle stability (Stormont et al., 1985; Tochigi et al., 2006). Stormont et al. (1985) reported that the articular surface accounted for 100% of version stability and 30% of stability in external–internal rotation for a 670 N applied axial load. The range of the torque applied manually was between 3.36 Nm and 3.98 Nm in their study which is greater than the 2.5 Nm limit set in the present study. Their lower reported articular contribution for external–internal rotation stability compared to our result (60%) may be due to this higher torque, which results in larger magnitudes of rotation and consequently, the contribution of the ligaments to ankle stability may increase. Tochigi et al. (2006) reported that the articular surface accounted for 70% of anterior/posterior stability, 50% of version stability and 30% of stability in external–internal rotation for a 600 N applied axial load. They measured contact stress in the tibiotalar articulation by a real-time contact-stress sensor. Contribution of articular geometry was calculated by analyzing the contact-stress changes due to secondary loading (anterior/posterior force, eversion/inversion torque, or external/internal rotation torque) with a computer model of ankle geometry. Their study did not include the effect of the talomalleolar articulations. These two studies (Stormont et al., 1985; Tochigi et al., 2006) and the current study analyzed contribution of joint structures to ankle stability. Conclusions from all three studies were consistent.

There are limitations of this study. The mean age of the cadaveric specimens was elderly and may not represent results from a younger population. Inversion–eversion stability was not included in our experimental protocol. Finally, we did not specifically examine the effects of muscle activity to stability were excluded or load the ankles dynamically.

Understanding the contribution of supporting elements to ankle stability is not only important in modeling the ankle and foot, but also is of importance clinically. Joint injuries such as displaced intraarticular fractures should be restored to anatomic alignment, in order to preserve joint stability. Insufficiency of the lateral and/or deltoid ligaments has an effect upon joint stability in multiple planes and efforts should be directed towards restoring normal ankle ligament function. Reconstruction of the ankle joint with total ankle arthroplasty is dependent upon successful restoration of ankle ligament stability. In the normal ankle, various ligaments and articular geometry interact to stabilize the joint for a wide range of loading and functional requirements. Injury or loss of supporting structures has the potential of disturbing functional stability. When primary joint stability is lost, impaired function may result. This study demonstrated the primary contribution that ankle geometry provided to stability of the ankle under physiologic loads.

In conclusion, there are many factors affecting stability of the ankle joint. There is no single factor that is most important. The contribution of each of these supporting elements is dependent upon the ground condition, loading level, the direction the forces applied and the degree of loading.

Conflict of interest statement

The authors have no conflict of interest regarding any of the material in the manuscript and meet the criteria for authorship as defined in the submission guidelines.

Acknowledgement

The support of a grant from the American Orthopaedic Foot and Ankle Society is gratefully acknowledged.

References

Bahr, R., Pena, F., Shine, J., Lew, W.D., Lindquist, C., Tyrdal, S., et al., 1997. Mechanics of the anterior drawer and talar tilt tests. A cadaveric study of lateral ligament injuries of the ankle. Acta Orthop. Scand. 68, 435–441.
Barnett, C.H., Napier, J.R., 1952. The axis of rotation at the ankle joint in man. Its influence upon the form of the talus and the mobility of the fibula. J. Anat. 86, 1–9.
Berglund, L.J., Samson, M., An, K.N., 1994. Four axial structural and material test machine. Biomed. Sci. Instrum. 30, 213–217.
Bulucu, C., Thomas, K.A., Halvorson, T.L., Cook, S.D., 1991. Biomechanical evaluation of the anterior drawer test: the contribution of the lateral ankle ligaments. Foot Ankle 11, 389–393.
Butler, D.L., Noyes, F.R., Grood, E.S., 1980. Ligamentous restraints to anterior–posterior drawer in the human knee. A biomechanical study. J. Bone Joint Surg. Am. 62, 259–270.
Cass, J.R., Settles, H., 1994. Ankle instability: in vitro kinematics in response to axial load. Foot Ankle Int. 15, 134–140.
Close, R., 1956. Some applications of the functional anatomy of the ankle joint. J. Bone Joint Surg. Am. 38, 761–781.
Glasgow, M., Jackson, A., Jamieson, A.M., 1980. Instability of the ankle after injury to the lateral ligament. J. Bone Joint Surg. Br. 62, 196–200.
Halder, A.M., Kuhl, S.G., Zobitz, M.E., Larson, D., An, K.N., 2001. Effects of the glenoid labrum and glenohumeral abduction on stability of the shoulder joint through concavity-compression: an in vitro study. J. Bone Joint Surg. Am. 83, 1062–1069.
Harper, M.C., 1987. Deltoid ligament: an anatomical evaluation of function. Foot Ankle 8, 19–22.
Harper, M.C., 1990. Talar shift. The stabilizing role of the medial, lateral and posterior ankle structures. Clin. Orthop. 257, 177–183.
Haugstvedt, J.R., Berger, R.A., Berglund, L.J., Neal, P.D., Sabick, M.B., 2002. An analysis of the constraint properties of the distal radioulnar ligament attachments to the ulna. J. Hand Surg. Am. 27, 61–67.
Hollis, J.M., Blasier, R.D., Flahiff, C.M., 1995. Simulated lateral ankle ligamentous injury. Change in ankle stability. Am. J. Sports Med. 23, 672–677.
Itoi, E., Lee, S.B., Berglund, L.J., Berge, L.L., An, K.N., 2000. The effect of a glenoid defect on anteroinferior stability of the shoulder after Bankart repair: a cadaveric study. J. Bone Joint Surg. Am. 82, 35–46.
Johnson, E.E., Markolf, K.L., 1983. The contribution of the anterior talofibular ligament to ankle laxity. J. Bone Joint Surg. Am. 65, 81–88.
Knutson, J.S., Kilgore, K.L., Mansour, J.M., Crago, P.E., 2000. Intrinsic and extrinsic contributions to the passive moment at the metacarpophalangeal joint. J. Biomech. 33, 1675–1681.
Larsen, E., 1986. Experimental instability of the ankle. A radiographic investigation. Clin. Orthop. 204, 193–200.
Liu, W., Maitland, M.E., Nigg, B.M., 2000. The effect of axial load on the in vivo anterior drawer test of the ankle joint complex. Foot Ankle Int. 21, 420–426.
Mack, R.P., 1982. Ankle injuries in athletics. Clin. Sports Med. 1, 71–84.
McCullough, C.J., Burge, P.D., 1980. Rotatory stability of the load-bearing ankle. An experimental study. J. Bone Joint Surg. Br. 62, 460–464.
Minami, A., An, K.N., Cooney III, W.P., Linscheid, R.L., Chao, E.Y., 1985. Ligament stability of the metacarpophalangeal joint: a biomechanical study. J. Hand Surg. Am. 10, 255–260.
Morrey, B.F., An, K.N., 1983. Articular and ligamentous contributions to the stability of the elbow joint. Am. J. Sports Med. 11, 315–319.
Rasmussen, O., 1985. Stability of the ankle joint. Analysis of the function and traumatology of the ankle ligaments. Acta Orthop. Scand. Suppl. 211, 1–75.
Rasmussen, O., Kromann-Andersen, C., Boe, S., 1983. Deltoid ligament. Functional analysis of the medial collateral ligamentous apparatus of the ankle joint. Acta Orthop. Scand. 54, 36–44.
Ritt, M.J., Bishop, A.T., Berger, R.A., Linscheid, R.L., Berglund, L.J., An, K.N., 1998. Lunotriquetral ligament properties: a comparison of three anatomic subregions. J. Hand Surg. Am. 23, 425–431.
Simonsen, E.B., Dyhre-Poulsen, P., Voigt, M., Aagaard, P., Sjogaard, G., Bojsen-Moller, F., 1995. Bone-on-bone forces during loaded and unloaded walking. Acta Anat. (Basel) 152, 133–142.
Stiehl, J.B., 1991. Inman's Joints of the Ankle. Williams & Wilkins, Baltimore.
Stiehl, J.B., Skrade, D.A., Needleman, R.L., Scheidt, K.B., 1993. Effect of axial load and ankle position on ankle stability. J. Orthop. Trauma 7, 72–77.
Stormont, D.M., Morrey, B.F., An, K.N., Cass, J.R., 1985. Stability of the loaded ankle. Relation between articular restraint and primary and secondary static restraints. Am. J. Sports Med. 13, 295–300.

Stuart, P.R., Berger, R.A., Linscheid, R.L., An, K.N., 2000. The dorsopalmar stability of the distal radioulnar joint. J. Hand Surg. Am. 25, 689–699.
Tochigi, Y., Rudert, J.M., Saltzman, C.L., Amendola, A., Brown, T.D., 2006. Contribution of articular surface geometry to ankle stability. J. Bone Joint Surg. Am. 88, 2704–2713.
Watanabe, K., Crevoisier, X.M., Kitaoka, H.B., Zhao, K.D., Berglund, L.J., Kaufman, K.R., et al., 2009. Analysis of joint laxity after total ankle arthroplasty: cadaver study. Clin. Biomech. 24, 655–660.
Waterman, B.R., Owens, B.D., Davey, S., Zacchilli, M.A., Belmont Jr., P.F., 2010. The epidemiology of ankle sprains in the United States. J. Bone Joint Surg. Am. 92, 2279–2284.
Yeung, M.S., Chan, K.M., So, C.H., Yuan, W.Y., 1994. An epidemiological survey on ankle sprain. Br. J. Sports Med. 28, 112–116.

Gait & Posture 37 (2013) 264–268

Contents lists available at SciVerse ScienceDirect

Gait & Posture

journal homepage: www.elsevier.com/locate/gaitpost

Posterior tibial tendon dysfunction and flatfoot: Analysis with simulated walking

Kota Watanabe [a,b], Harold B. Kitaoka [a], Tadashi Fujii [a], Xavier Crevoisier [a], Lawrence J. Berglund [a], Kristin D. Zhao [a], Kenton R. Kaufman [a], Kai-Nan An [a,*]

[a] Department of Orthopedic Surgery, Mayo Clinic, Rochester, MN, USA
[b] Department of Orthopedic Surgery, Sapporo Medical University School of Medicine, Sapporo, Japan

ARTICLE INFO

Article history:
Received 11 October 2011
Received in revised form 16 July 2012
Accepted 21 July 2012

Keywords:
Flatfoot
Kinematics
Simulator
Cadaver
Gait simulation

ABSTRACT

Many biomechanical studies investigated pathology of flatfoot and effects of operations on flatfoot. The majority of cadaveric studies are limited to the quasistatic response to static joint loads. This study examined the unconstrained joint motion of the foot and ankle during stance phase utilizing a dynamic foot–ankle simulator in simulated stage 2 posterior tibial tendon dysfunction (PTTD). Muscle forces were applied on the extrinsic tendons of the foot using six servo-pneumatic cylinders to simulate their action. Vertical and fore-aft shear forces were applied and tibial advancement was performed with the servomotors. Three-dimensional movements of multiple bones of the foot were monitored with a magnetic tracking system. Twenty-two fresh-frozen lower extremities were studied in the intact condition, then following sectioning peritalar constraints to create a flatfoot and unloading the posterior tibial muscle force. Kinematics in the intact condition were consistent with gait analysis data for normals. There were altered kinematics in the flatfoot condition, particularly in coronal and transverse planes. Calcaneal eversion relative to the tibia averaged 11.1 ± 2.8° compared to 5.8 ± 2.3° in the normal condition. Calcaneal-tibial external rotation was significantly increased in flatfeet from mean of 2.3 ± 1.7° to 8.1 ± 4.0°. There were also significant changes in metatarsal-tibial eversion and external rotation in the flatfoot condition. The simulated PTTD with flatfoot was consistent with previous data obtained in patients with PTTD. The use of a flatfoot model will enable more detailed study on the flatfoot condition and/or effect of surgical treatment.

1. Introduction

In recent years, there have been multiple reports related to posterior tibial tendon dysfunction (PTTD). PTTD is a common cause of acquired flatfoot deformity in adults; the condition may reach a prevalence of 10% in elderly women [1]. Most of the clinical investigations reported the effects of various operations to correct PTTD and flatfoot deformity, but *in vitro* and radiologic studies have also been published [2–5]. The optimum management of stage 2 PTTD [2] in which there is a mobile flatfoot has been a subject of debate for more than two decades. There are questions regarding the pathoanatomy of the deformity resulting from tendon dysfunction. A comprehensive understanding of the flatfoot malalignment will lead to more effective techniques for correcting it.

Previous investigators recognized the importance of defining the flatfoot and quantitating the degree of deformation [6]. Clinical measurements such as arch height have been used, but were not consistent between examiners [6]. Radiologic measurements of flatfoot have been performed in patients with PTTD [4,5]. Analysis of foot prints and ground reaction data in flatfeet have been reported [7]. Previous reports determined the contribution of various static elements in supporting the arch [8]. Others indicated that the posterior tibial tendon (PTT) plays a role in the dynamic support of the arch [3]. Most of these previous reports were *in vitro* studies with static loading of specimens. Recent gait analysis studies have revealed kinematics changes of the foot between normal and flatfoot [9–12]. *In vitro*, dynamic joint simulators have been developed recently for foot/ankle as well as other joints and applied for biomechanical studies of pathological situations of foot/ankle problems [13–19]. However, there have not been any publications, to our knowledge, detailing the three-dimensional kinematics of the flatfoot during simulated walking of the entire stance phase of gait.

We developed a dynamic foot–ankle simulator capable of recreating the stance phase of gait in cadaveric lower extremities [15]. It allows simulation of functional activities by allowing unconstrained motion of the foot and ankle while simultaneously applying time-histories of forces that affect the foot. A dynamic

* Corresponding author at: Mayo Clinic, 200 First Street SW, Rochester, MN 55905, USA. Tel.: +1 507 538 1717; fax: +1 507 284 5392.
E-mail address: an@mayo.edu (K.-N. An).

0966-6362/$ – see front matter © 2012 Elsevier B.V. All rights reserved.
http://dx.doi.org/10.1016/j.gaitpost.2012.07.015

simulator will be useful for improving our understanding of the mechanical behavior of the flatfoot compared to the normal foot. The purpose of the study was to examine unconstrained joint motion of the foot and ankle during stance phase in cadaveric lower extremities with simulated PTTD with flatfoot deformity utilizing a dynamic foot–ankle simulator.

2. Methods

Twenty-two fresh-frozen lower extremities were evaluated after gross visual screening for preexisting abnormalities of the foot. The mean age of the specimens was 78 years old (range, 47–95). Five were female, 17 male. Fourteen specimens were left feet and eight were right. The institutional research ethics committee reviewed and approved the study.

The custom simulator was able to subject cadaveric foot and ankle specimens to specified time-histories of normative ground reaction forces (GRF), and tendon loading based on physiological cross-sectional area (PCSA) and electromyography (EMG) data. Adjustments were made the initial muscle force profiles to match normal patterns of calcaneal-tibial angles and gross forefoot motion, while allowing totally unconstrained joint motions. The inputs were the forward tibial motion, fore-aft shear loading, tibial loading, and muscle loading. The outputs were measured foot reaction (force and center-of-pressure advancement) and joint kinematics. Since few biomechanical models were available for this hybrid (load and motion) control system, the tibial loading was prescribed to the normal vertical GRF profile as an approximation using a closed-loop servomotor so as to match the normal vertical GRF despite the disturbances from the muscle loading actuators. Ankle joint kinematics was controlled by muscle loading, which was initially targeted from the muscle gain, PCSA, and EMG data for each muscle group.

The leg specimen, amputated at the mid-tibial level, was potted in an acrylic plastic tube with polymethylmethacrylate cement, and fixed on the tendon loading unit (Fig. 1) [15]. The tendon-loading unit, consisting of six pneumatic cylinders, was connected through a linear ball screw to the servomotor tibial angle control unit, and through a hinge joint to the vertical loading unit. All the above units created a four-bar rocker configuration to control the angle of the loading unit or tibia relative to the ankle joint during the simulation. The vertical-loading unit, mounted on the frame, was connected to a linear slide powered by a linear ball screw and servomotor. This servomotor axis provided loading along the tibial axis by moving both the vertical loading unit and tendon loading unit onto the force plate. The sole of the foot contacted the custom-made force plate, which recorded the simulated vertical GRF. The bearing plate beneath the force plate allowed the relative forward translation of the foot and ankle and accommodated the anteroposterior shear force [20] by coupling the plate to another closed-loop servo axis. Most structures were built using non-metallic tubing or acrylic plastics, to minimize any interference with the magnetic tracking system.

The tibial angle control unit translated the tibial motion between 20° anterior and 40° posterior to vertical [21]. During testing, the tibial angle was monitored by a potentiometer. The tibial angle was used to determine the percentage of stance phase from the tibial angle history profile [21]. The estimated percent stance phase was used to prescribe the tendon and tibial loading [20,21]. The extrinsic muscles acting on or around the ankle were divided into six functional units: gastrocnemius-soleus, PTT, flexor hallucis longus-flexor digitorum longus, anterior tibial, extensor hallucis longus-extensor digitorum longus, and peroneus longus-peroneus brevis. A total of six pneumatic cylinders driven by servo-pneumatic valves were used to apply loads to the tendons. Sutures were attached to each tendon using a modified Krackow technique except for the Achilles tendon, which was sutured using a Leeds-Keio artificial ligament (Ellis Developments, Nottingham, UK) to sustain the comparable physiological loading. A uniaxial load cell was connected to each cylinder to monitor the load feedback signal to an IBM PC. A custom-written program (LabVIEW®, National Instruments, Austin, TX) was used for control and kinetic data acquisition. Tendon loads were estimated from PCSA and EMG data in the literature [20,22]. A linear EMG and force relationship was assumed [23,24]. An unknown muscle gain K and the corresponding cross sectional area (PCSAi) were multiplied by the relative EMG data (EMGi) to provide absolute forces to each cylinder ($Fi = K \times PCSAi \times EMGi$). To determine the unknown muscle gain or muscle stress, simulations were repeated until the gross foot–ankle kinematics matched reasonably well to the stance phase center-of-pressure and motion patterns, while the gain of the muscles was simultaneously adjusted. The applied vertical and fore-aft loads were reduced for the cadaver feet due to the limited suture strength and age of the specimens.

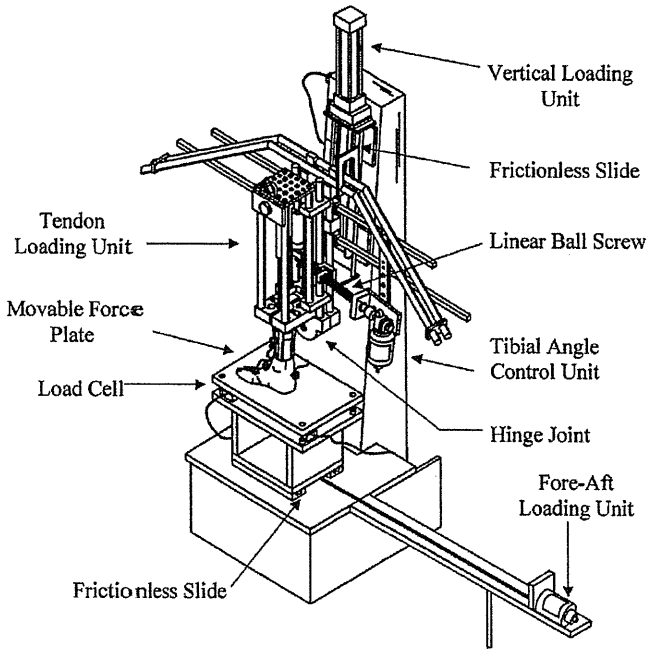

Fig. 1. Schematic drawing of the dynamic foot/ankle simulator.

Each specimen was cycled additional times through the entire stance phase to reduce the viscoelastic effect of soft tissues. The leg was then continuously moved from tibial flexion −20° (initial contact) to 40° flexion (pre-swing) while applying forces to the six muscle groups and subjecting it to the ground reaction force profiles. After testing the intact condition, a flatfoot condition was created by sectioning the peritalar soft tissue structures, including the spring ligament, long and short plantar ligaments, talocalcaneal interosseous ligament, medial talocalcaneal ligament, and tibionavicular portion of the superficial deltoid ligament. In order to simulate stage 2 PTTD and flatfoot, the posterior tibial muscle action was not simulated. A previous study [8] showed that flatfoot deformity occurred after these procedures, similar to that caused by stage 2 PTTD clinically. The applied vertical and fore-aft loads were not changed before and after the flatfoot model was created. Testing was performed three times for each condition and the average result was used for analysis.

Three-dimensional movements of the calcaneus and first metatarsus relative to the tibia were obtained with a magnetic tracking system (3Space Tracker System, Polhemus, Colchester, VT) [25,26]. The electromagnetic transmitter was fixed to the loading frame. Sensors were rigidly fixed to the anteromedial tibial diaphysis at the junction of the middle and distal thirds, posterolateral calcaneal body, and diaphysis of the dorsal-medial first metatarsal with acrylic mounting posts [26]. The relative angular motion between bones (calcaneal-tibial and first metatarsal-tibial) was expressed in terms of Eulerian angle description [25,26]. Bone positions were described relative to the previously described coordinate system [26]. The x-axis was oriented proximal-distal, the y-axis was oriented medial-lateral, and the z-axis was oriented anterior-posterior. The x-axis was along the tibial shaft through the ankle center, the z-axis was parallel to the projection of a line connecting the center of the heel and the second metatarsal on a plane perpendicular to the x-axis passing through the ankle center, and the y-axis was the product of the x- and z-axes following the right-hand rule passing through the ankle center. The three axes were also used to define the perpendicular planes: coronal (x–y plane), sagittal (x–z plane), and transverse (y–z plane). Motion was defined as inversion and eversion in the coronal plane, dorsiflexion and plantarflexion in the sagittal plane, and internal rotation and external rotation in the transverse plane.

Statistical analysis was performed with a paired t-test, comparing the bony positions in the intact and flatfoot conditions. The level of significance was set at $p < 0.05$.

3. Results

All the results of angular motions of the calcaneus and the first metatarsal relative to the tibia are presented over an entire stance phase that started with heel strike and ended with toe-off (Fig. 2). Angular movement patterns were consistent across all specimens. In the sagittal plane, the forefoot contacted with the force plate at about 10% stance phase. Maximum dorsiflexion was observed at about 80% stance phase. Then rapid plantarflexion occurred until maximum plantarflexion at toe-off. In the coronal plane, the hindfoot (calcaneal-tibial) and forefoot (metatarsal-tibial) moved from an initial inversion at heel strike to eversion. Maximum eversion occurred at a late phase of stance, prior to heel rise. Then the foot progressively inverted until toe-off. In the transverse plane, the hindfoot and forefoot moved from an initial internal rotation to external rotation. At mid-stance the foot reversed and began to internal rotate until toe-off.

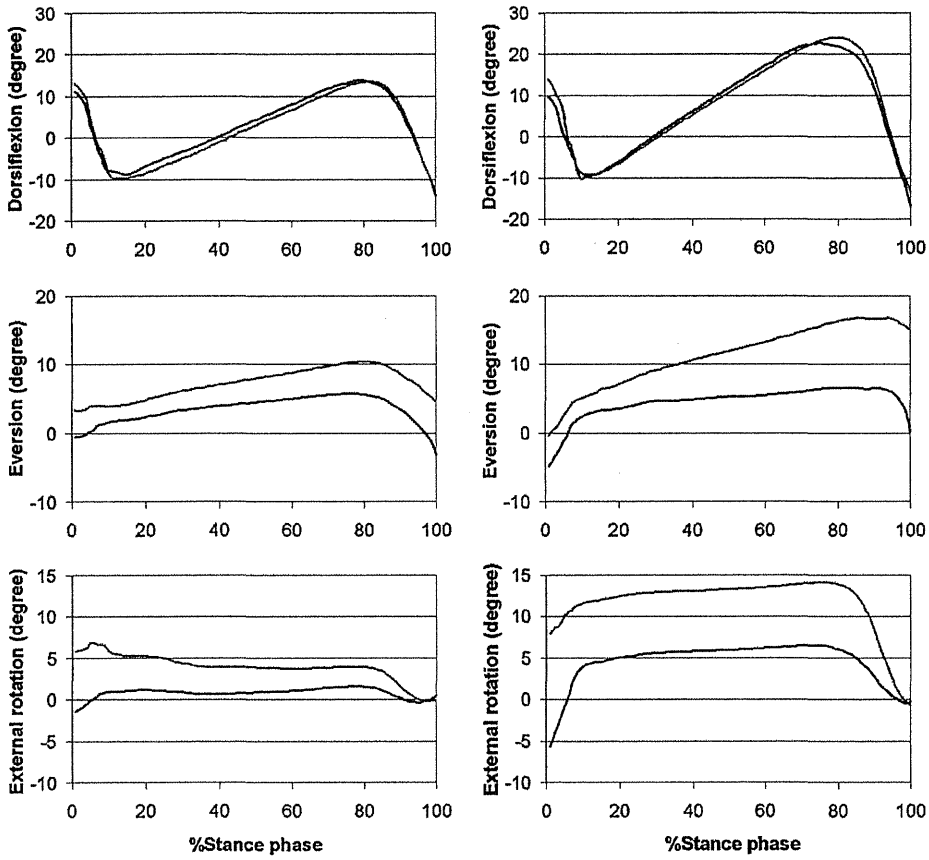

Fig. 2. Angular motions of the calcaneus (left) and the first metatarsal (right) relative to the tibia during the stance phase of walking in normal (black line) and flatfoot (gray line) conditions (mean ± SD). Positive and negative values indicate dorsiflexion and plantar flexion, eversion and inversion, and external rotation and internal rotation, respectively.

In the flatfoot, there was increased eversion and external rotation, but not dorsiflexion. The coronal plane motion curves demonstrated the characteristic inversion in late stance was absent in the flatfoot, in calcaneal-tibial and metatarsal-tibial motions. The transverse plane motions were also abnormal, as there was increased external rotation of the ankle-hindfoot (calcaneal-tibial) and forefoot (metatarsal-tibial). The typical internal rotation in late stance was not present in the flatfeet.

Calcaneal-tibial maximum dorsiflexion was 14.1 ± 4.1° (mean ± SD). In the flatfoot, maximum dorsiflexion was 14.4 ± 4.4° (not significant: NS). Calcaneal-tibial maximum eversion was 5.8 ± 2.3°. In the flatfoot, maximum eversion was 11.1 ± 2.8° (significant). Calcaneal-tibial maximum external rotation was 2.3 ± 1.7°. In the flatfoot, maximum external rotation was 8.1 ± 4.0° (significant) (Table 1).

Metatarsal-tibial maximum dorsiflexion was 24.8 ± 4.3°. In the flatfoot, maximum dorsiflexion was 25.5 ± 5.4° (NS). Metatarsal-tibial maximum eversion was 7.7 ± 4.2°. In the flatfoot, maximum eversion was 17.9 ± 6.1° (significant). Metatarsal-tibial maximum external rotation was 6.9 ± 3.5°. In the flatfoot, maximum external rotation was 15.3 ± 5.1° (significant) (Table 2).

Table 1
Calcaneal-tibial motion (mean ± SD).

	Normal	Flatfoot
Sagittal plane		
Max. plantarflexion at foot flat	10.9 ± 4.2	11.5 ± 4.4
Max. dorsiflexion	14.1 ± 4.1	14.4 ± 4.4
Max. plantarflexion at preswing	13.9 ± 8.0	12.6 ± 7.8
Total motion, foot flat to max. dorsiflexion	25.0 ± 5.1	25.9 ± 5.5
Total motion, max. dorsiflexion to preswing	28.0 ± 7.7	27.0 ± 7.3
Coronal plane		
Max. eversion	5.8 ± 2.3	11.1 ± 2.8*
Max. inversion	4.0 ± 4.0	-1.9 ± 2.4*
Total motion	9.8 ± 3.6	9.2 ± 2.9
Transverse plane		
Max. external rotation	2.3 ± 1.7	8.1 ± 4.0*
Max. internal rotation	2.8 ± 3.4	1.5 ± 3.7*
Total motion	5.1 ± 2.7	9.6 ± 3.8*

* Significantly different ($p < 0.05$).

Table 2
Metatarsal-tibial motion (mean ± SD).

	Normal	Flatfoot
Sagittal plane		
Max. plantarflexion at foot flat	14.2 ± 4.0	14.7 ± 3.7
Max. dorsiflexion	24.8 ± 4.3	25.5 ± 5.4
Max. plantarflexion at preswing	17.1 ± 9.8	13.3 ± 9.2*
Total motion, foot flat to max. dorsiflexion	39.0 ± 4.5	39.9 ± 5.4
Total motion, max. dorsiflexion to preswing	41.9 ± 8.6	38.5 ± 8.5*
Coronal plane		
Max. eversion	7.7 ± 4.2	17.9 ± 6.1*
Max. inversion	6.1 ± 5.9	0.3 ± 5.1*
Total motion	13.8 ± 6.9	18.2 ± 8.0*
Transverse plane		
Max. external rotation	6.9 ± 3.5	15.3 ± 5.1*
Max. internal rotation	7.7 ± 6.4	2.1 ± 6.3*
Total motion	14.6 ± 6.0	17.5 ± 5.1*

* Significantly different ($p < 0.05$).

4. Discussion

Flatfoot is a complex structural deformity which includes a decrease in the arch height, heel valgus, and forefoot abduction. The dynamic testing in this kinematics study demonstrated an increase in eversion and external rotation throughout most of stance phase. It also demonstrated the effects of the loss of posterior tibial muscle function as the typical pronounced inversion and internal rotation in late stance phase did not occur in simulated flatfoot gait. However, there still was some degree of motion toward inversion and internal rotation in toe-off, due to preservation of flexor digitorum longus, flexor hallucis longus, and gastrocnemius-soleus muscles which acted as secondary invertor [20]. The kinematics created *in vitro* were consistent with that observed clinically and radiologically, with forefoot external rotation and hindfoot eversion.

Several gait analysis studies have recently compared participants with flat feet to those with normal foot posture [9–12]. Levinger et al. [10] reported differences in foot motion between the two groups using a three-dimensional motion analysis system. Participants with flat feet demonstrated greater peak rearfoot eversion relative to the tibia (mean peak angular value of 5.8° *vs* 2.5°) and forefoot abduction relative to the rearfoot (mean peak angular value of 12.9° *vs* 1.8°), while similar rearfoot dorsiflexion/plantarflexion motion relative to the tibia compared with those with normal feet. The angular motion patterns of each foot segment during stance phase were similar between normal and flatfeet in the three planes. Tome et al. [11] reported the similar trend of foot motion changes with loss of arch height in flatfeet compared to normal. These findings were consistent with our results. The present study demonstrated that the changes in bone position during simulated walking in the flatfoot in stance phase approximated the *in vivo* condition.

The pathology and pathoanatomy associated with posterior tibial tendonitis and tendon dysfunction have been studied. Mosier et al. [27] examined the histologic changes in surgical specimens from patient who underwent operative procedures for PTTD and flatfeet. Radiologic studies of flatfeet have also been conducted [4,5]. Karasick [4] described the preoperative radiographic appearance of the acquired asymmetric flatfoot caused by a tear of PTT. These radiographic changes reflected the loss of tendon function and the development of a flatfoot deformity.

The disorder was examined experimentally in previous cadaveric testing. Chu et al. [3] performed a cadaver study to determine if the application of muscle forces simulating the midstance part of gait had an effect on flatfoot deformity measured evaluated radiographically. Changes in the talar-first metatarsal angle and the height of the medial cuneiform were noted. The authors concluded that, the medial structures (the spring ligament and possibly the plantar fascia) must be severed to create an effective flatfoot model and cyclical loading of the foot further increases flattening of the arch. In the present study, the planar fascia was not sectioned to create the flatfoot, as it was not felt to be ruptured in patients with PTTD.

Niki et al. [28] investigated the functional role of PTT in acquired flatfoot; intact (normal) specimens were loaded to simulate heel strike, stance, and heel rise, with and without PTT functioning. Subsequently, a procedure was performed on the specimens to create a simulated flatfoot deformity. The flattened feet were then used to determine the effect of restoring PTT function to a flatfoot model. Small, statistically significant changes in the angular positions of the hindfoot complex were observed between functional and dysfunctional PTT conditions. They concluded that the position of the foot could not be corrected by PTT as it had little effect in overcoming the soft tissue laxity. The present study demonstrated the value of dynamic testing as the effect of the flatfoot malalignment and loss of posterior tibial muscle function caused marked changes in the hindfoot alignment throughout the stance phase of gait.

A biomechanical evaluation of the foot and ankle should include the dynamic effects that may not be detectable in static measurement. Gait analysis can allow the investigation of important dynamic foot and ankle joint mechanics, but it is possible with cadaveric specimens to investigate internal parameters such as individual tarsal bone kinematics or soft tissue properties. The dynamic foot/ankle simulator will serve to study these internal parameters in normal and pathological conditions, and to study not only conventional but new treatment methods. Such investigations are obviously not ethical or possible in live subjects or patients.

There are several limitations of this study. First, it is not possible to simulate contraction of the intrinsic muscles of the foot. Secondly, the cadaveric specimens were elderly, and natural changes of foot posture and motion may exist with increasing age. Thirdly, full-scale normal ground reaction force loading was not applied to the cadaveric lower extremities as high loads may potentially affect suture fixation and soft tissue constraints with repeated testing. Further studies are needed to examine kinematics of the midfoot relative to the tibia or the calcaneus, and the calcaneus relative to the talus.

From the results of this study, we concluded that a simulator for the stance phase of walking was developed that which provided valid motions of the foot and ankle. The flatfoot deformity was associated with significant malalignment of the hindfoot (calcaneal-tibial) and forefoot (metatarsal-tibial) in multiple planes, throughout simulated stance phase of gait.

Acknowledgement

The support of the NIH R01 AR 42315 is gratefully acknowledged.

Conflict of interest statement

The authors have no conflicts to report.

References

[1] Kohls-Gatzoulis J, Angel JC, Singh D, Haddad F, Livingstone J, Berry G. Tibialis posterior dysfunction: a common and treatable cause of adult acquired flatfoot. British Medical Journal 2004;329:1328–33.
[2] Johnson KA, Strom DE. Tibialis posterior tendon dysfunction. Clinical Orthopaedics and Related Research 1989;239:196–206.
[3] Chu IT, Myerson MS, Nyska M, Parks BG. Experimental flatfoot model: the contribution of dynamic loading. Foot and Ankle International 2001;22:220–5.
[4] Karasick D, Schweitzer ME. Tear of the posterior tibial tendon causing asymmetric flatfoot: radiologic findings. American Journal of Roentgenology 1993;161:1237–40.
[5] Kitaoka HB, Patzer GL. Subtalar arthrodesis for posterior tibial tendon dysfunction and pes planus. Clinical Orthopaedics and Related Research 1997;187–94.
[6] Cowan DN, Robinson JR, Jones BH, Polly Jr DW, Berrey BH. Consistency of visual assessments of arch height among clinicians. Foot and Ankle International 1994;15:213–7.
[7] Bertani A, Cappello A, Benedetti MG, Simoncini L, Catani F. Flat foot functional evaluation using pattern recognition of ground reaction data. Clinical Biomechanics 1999;14:484–93.
[8] Kitaoka HB, Ahn TK, Luo ZP, An KN. Stability of the arch of the foot. Foot and Ankle International 1997;18:644–8.
[9] Hunt AE, Smith RM. Mechanics and control of the flat versus normal foot during the stance phase of walking. Clinical Biomechanics 2004;19:391–7.
[10] Levinger P, Murley GS, Barton CJ, Cotchett MP, McSweeney SR, Menz HB. A comparison of foot kinematics in people with normal- and flat-arched feet using the Oxford Foot Model. Gait and Posture 2010;32:519–23.
[11] Tome J, Nawoczenski DA, Flemister A, Houck J. Comparison of foot kinematics between subjects with posterior tibialis tendon dysfunction and healthy controls. Journal of Orthopaedic and Sports Physical Therapy 2006;36:635–44.

[12] Twomey D, McIntosh AS, Simon J, Lowe K, Wolf SI. Kinematic differences between normal and low arched feet in children using the Heidelberg foot measurement method. Gait and Posture 2010;32:1–5.
[13] Hurschler C, Emmerich J, Wulker N. In vitro simulation of stance phase gait. Part I. Model verification. Foot and Ankle International 2003;24:614–22.
[14] Iaquinto J, Adelaar RS, Wayne JS. Simulation of contact gait in the cadaveric lower extremity using a novel below knee simulator. Foot and Ankle International 2008;29:66–71.
[15] Kim KJ, Kitaoka HB, Luo ZP, Ozeki S, Berglund LJ, Kaufman KR, et al. In vitro simulation of the stance phase in human gait. Journal of Musculoskeletal Research 2001;5:113–21.
[16] Lee DG, Davis BL. Assessment of the effects of diabetes on midfoot joint pressures using a robotic gait simulator. Foot and Ankle International 2009;30:767–72.
[17] Nester CJ, Liu AM, Ward E, Howard D, Cocheba J, Derrick T, et al. In vitro study of foot kinematics using a dynamic walking cadaver model. Journal of Biomechanics 2007;40:1927–37.
[18] Sharkey NA, Hamel AJ. A dynamic cadaver model of the stance phase of gait: performance characteristics and kinetic validation. Clinical Biomechanics 1998;13:420–33.
[19] Whittaker EC, Aubin PM, Ledoux WR. Foot bone kinematics as measured in a cadaveric robotic gait simulator. Gait and Posture 2011;33:645–50.
[20] Perry J. Gait analysis. New Jersey: SLACK Incorporated; 1992.
[21] Inman VT, Ralston HJ, Todd F. Human walking. Baltimore: Waverly Press; 1981
[22] Dul J. Development of a minimum-fatigue optimization technique for predicting individual muscle forces during human posture and movement with application to the ankle musculature during standing and walking. PhD thesis. Nashville: Vanderbilt University; 1983.
[23] Perry J, Bekey GA. EMG–force relationships in skeletal muscle. Critical Reviews in Biomedical Engineering 1981;7:1–22.
[24] Woods JJ, Bigland-Ritchie B. Linear and non-linear surface EMG/force relationships in human muscles. An anatomical/functional argument for the existence of both. American Journal of Physical Medicine 1983;62:287–99.
[25] An KN, Jacobsen MC, Berglund LJ, Chao EY. Application of a magnetic tracking device to kinesiologic studies. Journal of Biomechanics 1988;21:613–20.
[26] Kitaoka HB, Lundberg A, Luo ZP, An KN. Kinematics of the normal arch of the foot and ankle under physiologic loading. Foot and Ankle International 1995;16:492–9.
[27] Mosier SM, Pomeroy G, Manoli 2nd A. Pathoanatomy and etiology of posterior tibial tendon dysfunction. Clinical Orthopaedics and Related Research 1999;12–22.
[28] Niki H, Ching RP, Kiser P, Sangeorzan BJ. The effect of posterior tibial tendon dysfunction on hindfoot kinematics. Foot and Ankle International 2001;22:292–300.

整・災外 56：1509—1512，2013

臨床

トモシンセシスを用いた遠位脛腓靱帯結合荷重撮影

寺本篤史[*1)] 渡邉耕太[*1)]
山下敏彦[*1)] 高島弘幸[*2)]

要旨：トモシンセシスはflat panel detectorを活用したデジタル断層撮影である。任意の断層面を再構成することが可能で負荷条件下での撮影も行えることから，整形外科分野への応用が進んでいる。本研究では荷重条件での遠位脛腓靱帯結合のトモシンセシス撮影を行い，その有用性を検討した。15名の健常被験者（平均年齢33.5±7.8歳，男性12名，女性3名）において臥位と立位での足関節冠状断トモシンセシス撮影を行い，遠位脛腓関節が確認できる断層像にて，脛骨天蓋レベルでの遠位脛腓間距離を計測した。計測値は臥位と立位の2条件間で比較検討した。トモシンセシスにより全症例で遠位脛腓関節の評価が可能であった。遠位脛腓間距離は臥位で平均3.1±0.9 mm，立位で平均3.8±0.9 mmであり，両群間に有意差を認めた（$p<0.001$）。本研究の結果から，トモシンセシスにより脛腓靱帯結合の荷重による開大の評価が可能であり，遠位脛腓靱帯損傷などの評価に応用可能であると考えられた。

はじめに

足関節外傷において，遠位脛腓靱帯結合損傷は足関節外側靱帯損傷に比べ発生頻度が低い。しかし，スポーツ外傷の増加と，この損傷に対する認識が高まっていることから，近年の報告ではその発生頻度が増加している[1)~3)]。また，遠位脛腓靱帯結合損傷は診断が比較的難しく，足関節外側靱帯損傷として治療されている場合があり，疼痛遷延の原因となることがある。遠位脛腓靱帯結合損傷の診断においては，理学所見のほかに単純X線撮影による果間関節窩の評価が行われている。果間関節窩撮影法（mortise view）では，足部を15°～20°内旋し撮影することで遠位脛腓関節が描出される[4)]。遠位脛腓関節は外旋ストレスや荷重負荷，足関節背屈負荷で生理的に開大するが，遠位脛腓靱帯損傷によって脛腓間距離は，より拡大する[5)]。しかし，単純X線像では，撮影条件やストレス肢位によって脛骨と腓骨の重なりが変化するため，遠位脛腓関節を正確に評価できない場合がある。一方，CTは遠位脛腓関節の描出が明瞭であるが，荷重やストレス条件での撮影が困難である。また，金属が存在すると，そのアーチファクトが画像評価に悪影響を及ぼすという難点がある。

トモシンセシスはX線平面検出器であるflat panel detector（FPD）を活用したデジタル断層撮影であり，任意の断層面を再構成することが可能

*1) Atsushi TERAMOTO et al，札幌医科大学医学部，整形外科学教室
*2) Hiroyuki TAKASHIMA，札幌医科大学附属病院，放射線部

Tomosynthesis imaging of distal tibiofibular syndesmosis

Key words：Tomosynthesis, Syndesmosis, Load
投稿 2013.5.22　再投稿 2013.7.9　採用 2013.7.16

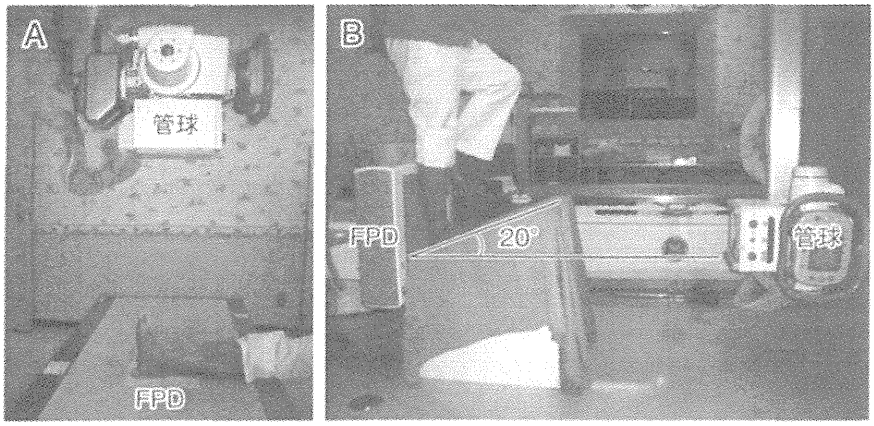

臥　位　　荷重背屈位

図 1　足関節トモシンセシス撮影肢位

である。また，ストレス負荷の条件下でも撮影が可能であり，整形外科分野への応用が進んでいる[6]。以上から，トモシンセシスは遠位脛腓靱帯結合の評価に有用である可能性があるが，渉猟し得た限りトモシンセシスをこの領域に応用した報告はない。

本研究の目的は，荷重条件での足関節トモシンセシス撮影を行い，遠位脛腓靱帯結合の生理的開大を評価し，トモシンセシスの有用性を検討することである。

Ⅰ．対象と方法

対象は足部に外傷の既往がない健常ボランティア 15 名である。平均年齢は 33.5±7.8 歳で男性が 12 名，女性が 3 名であった。GE 社製 Discovery XR650 を用いて足関節冠状断トモシンセシス撮影を行った。撮影条件は断層振り角 40°（平行走査），管電圧 60 kV，管電流 160 mA とした。撮影したデータは filter back projection method で再構成した。撮影肢位は臥位と荷重位の 2 条件とした。臥位では被験者が FPD に足部を載せ，管球を上方に設置し撮影した。荷重位では被験者が 20° の楔状台で片脚立位をとり，足関節背屈 20° で全荷重負荷となるようにし，管球を前方に設置し撮影した（図 1）。撮影したデータは Ziosoft 社画像解析ソフト zioTerm を用いて計測した。計測は冠状断中央スライスで遠位脛腓関節が明瞭に確認できる断層像を選択し，脛骨天蓋レベルでの遠位脛腓間距離を計測した（図 2）。臥位，荷重背屈位ともに同スライスを採用し，脛腓間距離の計測を行った。計測値の統計学的解析として，臥位と荷重背屈位の 2 条件間で対応のある t 検定を行い，p 値 0.05 未満で有意差ありとした。

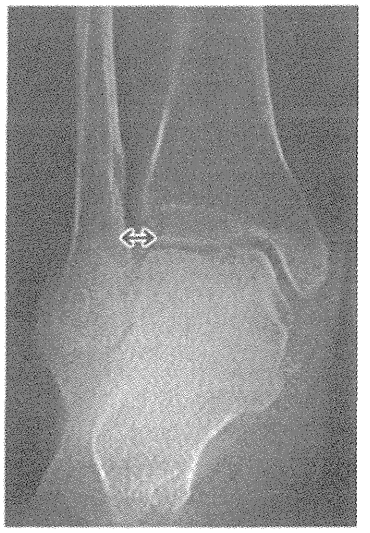

図 2　遠位脛腓間距離の計測部位（矢印）

Ⅱ．結　　果

全症例で臥位，荷重背屈位ともにトモシンセシスによって遠位脛腓関節の評価が可能であった。遠位脛腓間距離は臥位で平均 3.1±0.9 mm，立位

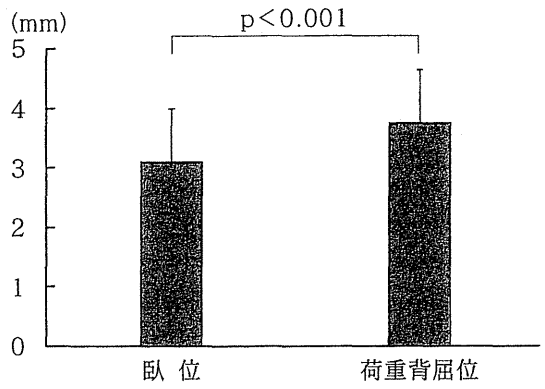

図 3 臥位と荷重背屈位での遠位脛腓間距離

で平均3.8±0.9 mmと増加した。両群間に統計学的有意差を認めた（p<0.001；図3）。

Ⅲ. 考　察

本研究では，トモシンセシスによって遠位脛腓関節の評価が可能であり，その開大は荷重によって平均0.7 mmの増加を認めた。

トモシンセシスは1回の断層撮影で任意の断層像を得ることが可能であり，FPDによって低歪み，視野拡大が得られ，新しい再構成手法の導入によって臨床応用が広がっている[6]。整形外科領域におけるトモシンセシスは，荷重やストレスなど負荷条件での機能的断層撮影が可能であること，金属アーチファクトの影響を受けにくいことなどの特徴がある[7]。照射線量はX線の3～5倍であるが[6]，CTと比較すると被曝線量低減，検査時間短縮といった利点がある[8]。複数の骨が重なり合う足関節や足部においては，単純X線像と比較してトモシンセシスは各関節の描出が明瞭で，荷重やストレス撮影による有用性も高いと考えられる。本研究では，トモシンセシスを用いて遠位脛腓靱帯結合の機能撮影を試みた結果，遠位脛腓関節が明瞭に描出可能であった。そして，健常者において遠位脛腓靱帯結合の背屈荷重時には生理的に開大が生じ，その量は平均0.7 mm程度であることがわかった。

健常者の遠位脛腓靱帯結合の生理的開大に関しては様々な報告がある。筆者らは過去にCTを用いた機能撮影を行い，足関節中間位撮影と比較して足関節最大背屈位撮影では遠位脛腓関節が平均0.6 mm開大したことを報告した[9]。また，未固定凍結人体標本を用いたバイオメカニクス研究では，電磁場センサーで離開距離計測を行った結果，足関節中間位に比べ足関節背屈位では平均0.4 mm開大した[10]。Radiostereometryで計測した研究では，足関節背屈負荷にて平均0.81 mmの開大が報告されている[11]。本研究では，過去の異なる研究方法の結果と同程度の生理的開大を認めた。

本研究には，いくつかの問題点がある。まずトモシンセシス撮影そのものの精度が不明である。スライス幅が約1～2 mmであるため，距離計測において誤差が生じている可能性がある。また画像解析ソフトにおける計測誤差や検者間，検者内計測誤差も考慮される必要がある。次に，健常者を対象としているが小児や高齢者が含まれておらず，また男女による開大量の違いなどは不明である。

本研究から，トモシンセシスによって遠位脛腓関節が明瞭に描出され，健常者の生理的な遠位脛腓靱帯結合開大評価が可能であることがわかった。本法による評価を臨床応用するためには，今後は遠位脛腓靱帯損傷足を対象に撮影を行い，荷重による開大量変化や健常者との比較検討が必要である。また，回旋ストレスなどの様々な負荷条件の影響や中足部，後足部のトモシンセシス撮影の有用性も評価検討していきたい。

文　献

1) Boytim MJ et al：Syndesmotic ankle sprains. Am J Sports Med **19**：294—298, 1991
2) Gerber JP et al：Persistent disability associated with ankle sprains；a prospective examination of an athletic population. Foot Ankle Int **19**：653—660, 1998
3) Wright RW et al：Ankle syndesmosis sprains in National Hockey League players. Am J Sports Med **32**：1941—1945, 2004
4) Takao M et al：Computed tomographic evaluation of the position of the leg for mortise radiographs. Foot Ankle Int **22**：828—831, 2001
5) Xenos JS et al：The tibiofibular syndesmosis；